

# Numerical Investigation of Ionization and Acceleration Processed in a Self-Field MPD Thruster

IEPC-2005-089

*Presented at the 29<sup>th</sup> International Electric Propulsion Conference, Princeton University,  
October 31 – November 4, 2005*

Kubota, K.\*

*Tokyo Institute of Technology, Yokohama, Kanagawa, 226-8503, Japan*

Funaki, I.†

*Japan Aerospace Exploration Agency, Sagami-hara, Kanagawa, 229-8510, Japan*

*and*

Okuno, Y.‡

*Tokyo Institute of Technology, Yokohama, Kanagawa, 226-8503, Japan*

**Abstract:** Numerical simulation code for the analyses in the wide operation range of a self-field magnetoplasmadynamic(MPD) thruster is developed. Argon is used as the propellant and non-equilibrium multiple ionization processes are considered for modeling of the high temperature plasma. To simulate a transition from electrothermal acceleration to electromagnetic acceleration, the discharge current is varied in the wide range from 3000A to 9000A under the mass flow rate 0.8 g/s. As a result, when the current increases up to 6000A, which corresponds to the theoretical value of critical ionization current, mass fraction of singly-ionized argon becomes dominant; also at this discharge current, the slope of the discharge voltage abruptly changes. In the last of paper, highly ionized and accelerated flow field above the critical condition is characterized, and rapid decrease of the electron number density is found in the range of electromagnetic acceleration.

## Nomenclature

$z$	= axial coordinate
$r$	= radial coordinate
$\rho$	= mass density (kg/m <sup>3</sup> )
$\mathbf{u}$	= velocity (m/s)
$p$	= pressure (N/m <sup>2</sup> )
$\mathbf{p}$	= pressure tensor
$\Pi$	= viscous stress tensor
$\mathbf{j}$	= current density (A/m <sup>2</sup> )
$\mathbf{B}$	= magnetic flux density (T)

---

\* Graduate student, Department of Energy Science, g04m3115@es.titech.ac.jp

† Assistant Professor, Institute of Space and Astronautical Science, funaki@isas.jaxa.jp

‡ Professor, Department of Energy Science, yokuno@es.titech.ac.jp

$\varepsilon$	= energy density (J/m <sup>3</sup> )
$\mathbf{E}$	= electric field (V/m)
$\lambda$	= thermal conductivity
$T$	= temperature (K)
$\Phi$	= dissipation function
$\mu_0$	= permeability
$\sigma$	= electrical conductivity (S/m)
$k_B$	= Boltzmann constant
$C_{i,e}$	= thermal velocity of ions, electron (m/s)
$n_{e,s}$	= number density of electron or heavy particle s (1/m <sup>3</sup> )
$Q_{ij}$	= collision cross section between i, j
$\dot{m}$	= mass flow rate (g/s)
$J$	= discharge current (A)
$V_i$	= ionization energy (J)
$M$	= mass of atom (kg)
$r_{a,c}$	= radius of anode, cathode (m)
$e$	= elementary charge (C)

## I. Introduction

NASA is developing a nuclear power generating system that could ultimately be used for a manned mission to Mars. A self-field magnetoplasmadynamic (MPD) thruster is one of the electric propulsion candidates suitable for such a mission. High-power MPD thrusters are intensively studied in the U.S., in ESA countries, and in Japan.<sup>1</sup>

The feature of the self-field MPD thruster is the acceleration of the plasma by the Lorentz force by the discharge current and the induced magnetic field. Since both ionization and acceleration occur in the same chamber, physical phenomena in the thruster are very complicated hence it is difficult to obtain the comprehensive information to optimize the performance. Our goal is, therefore, to model and simulate the processes in the MPD thruster for obtaining some design guidelines for high-power interplanetary missions.

Many theoretical studies have been underway in the research of MPD thruster using numerical simulation of the plasmas in the discharge chamber.<sup>2-5</sup> In the Institute of Space and Astronautical Science, two dimensional MPD thruster had been researched numerically and experimentally in order to examine the internal flow field.<sup>6</sup> Recently, axisymmetric MPD thrusters are examined experimentally for the optimization of the configuration.<sup>7</sup> However, since the observations of the internal plasma flows are difficult due to its configuration, numerical examination has to be conducted for the detailed understanding of the plasma in the various MPD thrusters. Then the purpose of this study is to develop a robust and useful MHD code in order to examine the plasma flow in the axisymmetric MPD thruster for the wide range of electric power. It is known that the thrust efficiency of a MPD thruster rises with increasing input power. However the performance is limited by the oscillation of the discharge voltage referred to as "Onset" when the discharge current is increased. The understanding and overcoming of the phenomenon will lead to realization of high performance thrusters. Therefore it is necessary to analyze the magnetohydrodynamic behavior in the range of high electric power, in particular where the electromagnetic acceleration is dominant. In this paper, the discharge current is varied in the wide range from 3000 to 9000 A where the mass flow rate  $\dot{m}$  is fixed to 0.8g/s in order to confirm whether the developed code can capture the essential features of the transition from the electrothermal acceleration to the electromagnetic acceleration. The maximum  $J^2/\dot{m}$  parameter is more than  $1 \times 10^{11}$  A<sup>2</sup>/kg/s, hence the analyses are conducted in the challenging range of operation. From the results, detailed examination as to the transition of the acceleration mode is performed. In addition, the decrease of electron number density is discussed in the range of electromagnetic acceleration in the last of this paper.

## II. Physical Modeling

The calculation region is depicted and the governing equations used for calculations in a self-field MPD thruster are discussed. In addition, boundary conditions imposed in this study are also shown. The input parameters are mass flow rate  $\dot{m}$ , inlet temperature, and discharge current  $J$ . In this study, the mass flow rate and inlet temperature are fixed to 0.8 g/s, and  $10^4$  K respectively, and the discharge current is changed from 3000A to 9000A.

### A. Calculation Region

Figure 1 shows the configuration of a thruster in this calculation. A flared anode and a short cathode are adopted. The radius of the cathode is 4mm. The radius of the anode is 14mm at the inlet and 27mm at the outlet. The axial length of the cathode and anode is 12mm and 59mm respectively.

### B. Governing equations

The governing equations used in this study are conservation equations of mass, momentum, energy, mass of ions, and inductive equation of magnetic field. Some assumptions are as follows. The propellant is argon, and all ionizations are caused by electron impact. As to ionization, non-equilibrium multiple ionization processes including up to  $\text{Ar}^{6+}$  are considered. The plasma flow is axisymmetric, electrically neutral, and in thermal equilibrium. Hall effect is not taken into account.

Mass conservation

$$\frac{\partial \rho}{\partial t} + \nabla \cdot \rho \mathbf{u} = 0 \quad (1)$$

Momentum conservation

$$\frac{\partial \rho \mathbf{u}}{\partial t} + \nabla \cdot (\rho \mathbf{u} \mathbf{u} + \mathbf{p}) = \nabla \cdot \Pi + \mathbf{j} \times \mathbf{B} \quad (2)$$

Energy conservation

$$\frac{\partial \varepsilon}{\partial t} + \nabla \cdot (\varepsilon + p) \mathbf{u} = \mathbf{j} \cdot \mathbf{E} + \nabla \cdot (\lambda \nabla \cdot T) + \Phi \quad (3)$$

Mass of ions

$$\frac{\partial \rho_s}{\partial t} + \nabla \cdot \rho_s \mathbf{u} = \dot{\rho}_s \quad (s=1 \sim 6) \quad (4)$$

Induction equation of magnetic field

$$\nabla \times (\mathbf{u} \times \mathbf{B}) - \nabla \times \left( \frac{1}{\mu_0 \sigma} \nabla \times \mathbf{B} \right) = 0 \quad (5)$$

where  $\Pi$  and  $\varepsilon$  denotes viscous stress tensor and energy density including ionization energy respectively. The  $ij$  component of the viscous stress tensor is given as

$$\Pi_{ij} = \mu \left[ \left( \frac{\partial u_i}{\partial x_j} + \frac{\partial u_j}{\partial x_i} \right) - \frac{2}{3} \delta_{ij} \frac{\partial u_k}{\partial x_k} \right] \quad (6)$$

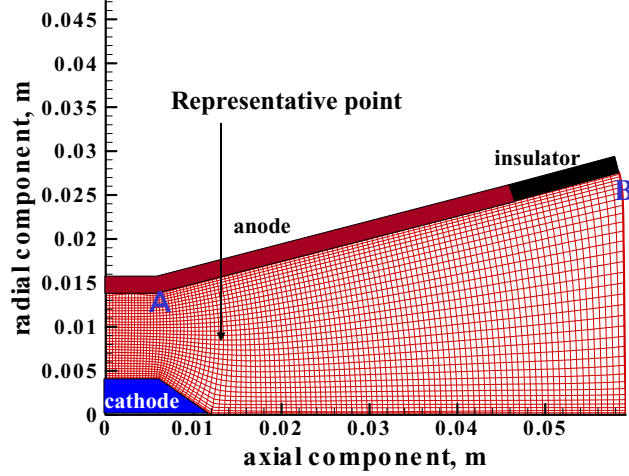


Figure 1. Calculation region

Since only steady flows are discussed in this paper, the steady induction equation of the magnetic field is adopted. Therefore the system equation of fluid and a steady induction equation of the magnetic field are solved alternatively. The other equations are Maxwell equation, Ohm's law, and state equation.

Maxwell equation

$$\nabla \times \mathbf{B} = \mu_0 \mathbf{j} \quad (7)$$

Ohm's law

$$\mathbf{j} = \sigma(\mathbf{E} + \mathbf{u} \times \mathbf{B}) \quad (8)$$

State equation

$$p = n_n k_B T + \sum_s n_s k_B T + n_e k_B T \quad (9)$$

The thermal conductivity  $\lambda = \lambda_e + \lambda_h$ , viscosity coefficient  $\mu$  and electrical conductivity  $\sigma$  are given, respectively, as<sup>8-10</sup>

$$\lambda_e = \frac{15k_B C_e}{8\sqrt{2}} \frac{n_e}{n_e Q_{ee} + \sqrt{2} \sum_s n_s Q_{es}} \quad (10)$$

$$\lambda_h = \frac{15k_B C_h}{8\sqrt{2}} \sum_{s \neq e} \frac{n_s}{\sum_{r \neq e} n_r Q_{sr}} \quad (11)$$

$$\mu = \frac{m_h C_h}{2\sqrt{2}} \sum_{s \neq e} \frac{n_s}{\sum_{r \neq e} n_r Q_{sr}} \quad (12)$$

$$\sigma = \frac{3}{8} \sqrt{\frac{\pi}{2}} \frac{e^2 n_e}{\sum_{s \neq e} n_s Q_{es} \sqrt{m_{es} k_B T}} \quad (13)$$

In the Eq.(4),  $\dot{\rho}_s$  denotes the formation ratio of ion  $s$ . The forward reaction coefficients are given by Lotz formula<sup>11-13</sup> which is valid for the ionization in the high temperature plasmas.

### C. Numerical Method

In this study, to avoid complicated schemes, the second order accurate in time and in space high-resolution Lax-Friedrich scheme is used.<sup>14-15</sup> This method does not require the calculation of eigenvector matrices which often appears in the general TVD schemes, thus it is useful for solving the MHD equations even if additional effects such as ionization is included in the model. The inductive equation of magnetic field can also be incorporated easily in the system equation with this scheme. In this study, however, the steady inductive equation is solved because the discussions are conducted for the steady state flows. Therefore Eq.(5) is solved every time step with SOR method.

### D. Boundary Conditions

At the inlet, the mass flow rate  $\dot{m}$  and the temperature are fixed to 0.8 g/s and  $10^4$  K respectively. The density and axial velocity are adjusted respectively at each grid to keep  $\dot{m}$  constant. The pressure gradient is set to zero and the ionization fraction is given by the Saha equation, where it is assumed that only single ionization occurs at the inlet. The magnetic flux density is determined from the Ampere's law.

$$B_{inlet} = \frac{\mu_0 J}{2\pi r} \quad (14)$$

The wall is assumed as adiabatic and the slip condition is used there. Although these conditions are unrealistic, it seems that the significant property of the main stream in the thruster can be examined with these conditions. As to the magnetic flux density along the wall, it is determined from the condition that the tangential component of the electric field is zero. On the insulator, the magnetic flux density is set to zero.

### III. Results and Discussion

Calculation in the wide range of discharge current is performed. In this section, the results of flow fields are shown and the performance is discussed in terms of thrust, specific impulse, and voltage. In addition, electron number density along the flared part of the anode is examined which may relate with the onset phenomenon.

According to many past arguments on the physics in MPD thrusters, critical ionization current  $J_{cr}$  is often used as a parameter to estimate the discharge current where the ionization processes progress rapidly.

$$J_{cr} = (\dot{m}u_{cr} / b)^{1/2} \quad (15)$$

where  $u_{cr} = (2V_i / M)^{1/2}$  is the critical ionization velocity, and  $b$  is a performance parameter given as

$$b = \frac{\mu_0}{4\pi} \left( \ln \frac{r_a}{r_c} + \frac{3}{4} \right) \quad (16)$$

In this study, the critical ionization current is about 6000 A, where the anode radius  $r_a$  is taken at its root.

#### E. Flow Field & Mass Fraction of Ions

To understand the typical flow field in the MPD thruster, the results of flow field analyses are shown in the case of  $J=6000$  A corresponding to the critical ionization current.

Calculated current distribution for a given current of 6000 A is illustrated in Fig. 2. Since the temperature is fixed to  $10^4$  K at the inlet, i.e., the ignition of plasma is not strictly considered, the current flows into cathode side even at the inlet. The discharge current tends to concentrate at the convex point of the cathode. In this study, a conic cathode head is adopted for the ease of generating mesh, but the part has to be hemispherical in terms of the problem arising from thermal erosion. The current contour lines extend toward the downstream as the discharge current increases due to the effect of the convection.

Figure 3 shows the temperature distribution. The temperature increased by the Joule heating diffuses overall in the thruster due to the effect of the thermal conduction. Highest temperature is about 6.4 eV at the cathode tip. When this value 6.4 eV is substituted for the equation to estimate the relative velocity between an atom and an ion whose distribution function is assumed as Maxwellian,

$$v_{in} = \sqrt{\frac{8k_B T}{\pi m_{in}}} \quad (17)$$

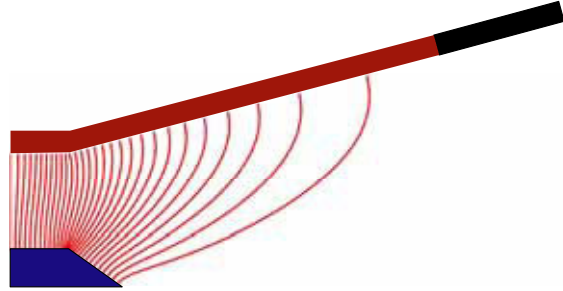
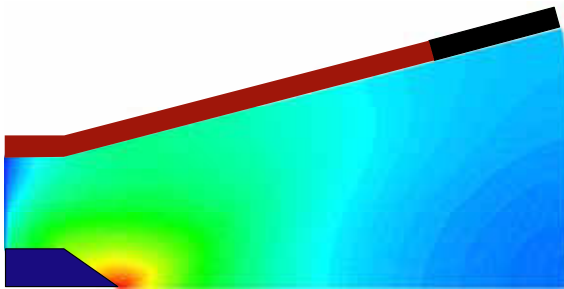
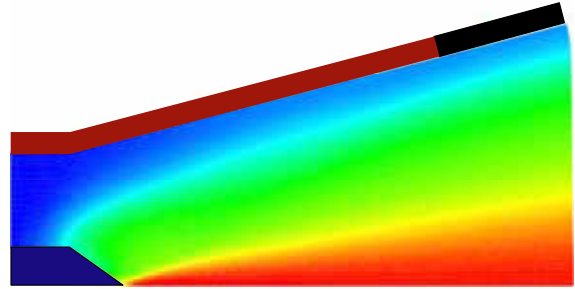


Figure 2. Current contour line (J=6000 A, mass flow rate 0.8 g/s)



0.9 1.6 2.3 3.0 3.7 4.4 5.0 5.7 6.4 eV

Figure 3. Temperature (J=6000 A, mass flow rate 0.8 g/s)



0.1 0.3 0.5 0.7 0.9 1.1 1.2 1.4 1.6

Figure 4. Ionization fraction (J=6000 A, mass flow rate 0.8 g/s)

where the unit of  $T$  is Kelvin and  $m_{in}$  denotes the reduced mass, it is shown that the relative velocity is equal to 8.8 km/s. It is notable that the critical ionization velocity of argon which is related with initiation of the single ionization is equal to 8.7 km/s. This fact is consistent with the argument that the critical ionization current derived from Eq.(15) is about 6000 A

Ionization fraction distribution is shown in Fig. 4. It is assumed that only single ionization occurs at the inlet, where the ionization fraction is given by the Saha equation. In the region of downstream, the ionization fraction distribution is divided into three regions. First one is the region near the anode where the ionization fraction is about 0.5. The second one is the middle region of the thruster where the ionization fraction is about 0.9. The plasma in this region is produced at the conic part of the cathode where the Joule heating is intensive. The third region is located along the symmetric axis. Plasma jet keeping high ionization fraction about 1.6 is obtained, namely cathode jet including  $Ar^{2+}$  is generated. Due to the compression to the cathode tip, the collision processes progress rapidly and many divalent ionization occurs.

The mass fraction of Ar,  $Ar^+$ , and  $Ar^{2+}$  at a representative point shown in the Fig. 1, which is located at  $z = 12.4$  mm,  $r = 8.5$  mm, is plotted in Fig.5 as a function of the discharge current. At  $J = 5000$  A, the mass fraction of Ar and  $Ar^+$  is approximately equal. Although the ratio of increment in  $Ar^+$  is not so rapid one which is expected from the theory of critical ionization velocity, it is notable that the fraction of  $Ar^+$  becomes the highest at  $J = 6000$  A. The fraction of  $Ar^{2+}$  begins to rise around  $J = 7000$  A and it exceeds the fraction of Ar at  $J = 9000$  A. Then the fraction of  $Ar^+$  decreases at  $J = 9000$  A due to the multiple ionization

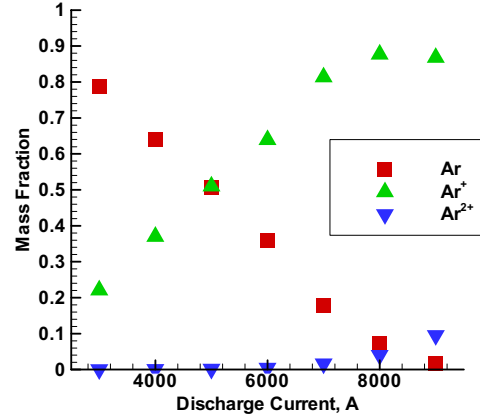


Figure 5. Mass fraction of Ar,  $Ar^+$ ,  $Ar^{2+}$  at a representative point ( $z=12.4$ mm,  $r=8.5$ mm)

## F. Thrust & Specific Impulse

The calculated thrust is shown in Fig. 6. The thrust is equal to the momentum flux at the outlet of the thruster. The thrust of an MPD thruster is divided into aerodynamic thrust and magnetic thrust. The magnetic thrust is given by the volume integral of the Lorentz force.

$$Thrust = \int_{outlet} (\rho u^2 + p) dS \quad (18)$$

$$Magnetic\ thrust = \int_V \mathbf{j} \times \mathbf{B} dV \quad (19)$$

The relation between the aerodynamic and magnetic thrust can be also understood with Fig. 6. The magnetic thrust exceeds the aerodynamic one at  $J = 6000$  A, namely when  $J$  is equal to critical ionization current, and it becomes dominant in the range of higher current. On the other hand, it is found that the aerodynamic thrust increases slightly with rising current in the range of  $J = 3000$  to  $5000$  A, and decreases gradually in the range of  $J > 5000$  A. To understand this property, energy balance between the work by the Lorentz force and Joule heating which is related with aerodynamic thrust is shown in Fig. 7. This figure shows input power as a function of the discharge current. The input power is defined as follows.

$$input\ power = \int_V \mathbf{j} \cdot \mathbf{E} dV = \int_V \left( \frac{\mathbf{j}^2}{\sigma} + \mathbf{u} \cdot (\mathbf{j} \times \mathbf{B}) \right) dV \quad (20)$$

In reality, total input power includes the sheath drop energy. Hence Eq.(20) denotes the energy putted just in the fluids. The ratio between the two terms in Eq.(20) is determined from a dimensionless number, that is magnetic Reynolds number. In the range of  $J = 3000$  to  $5000$  A, increasing amount of Joule heating is higher than the one of work by the Lorentz force. On the other hand, in the range of  $J > 5000$  A, the increasing amount of work by the

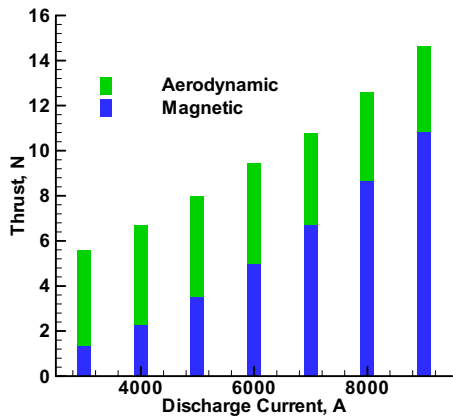


Figure 6. Thrust as a function of current (mass flow rate 0.8 g/s)

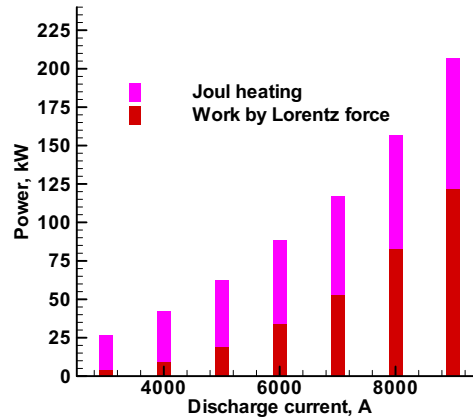


Figure 7. Power balance as a function of current (mass flow rate 0.8 g/s)

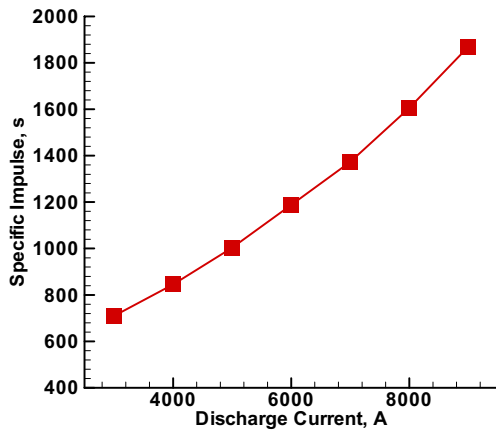


Figure 8. Specific Impulse as a function of current (mass flow rate 0.8 g/s)

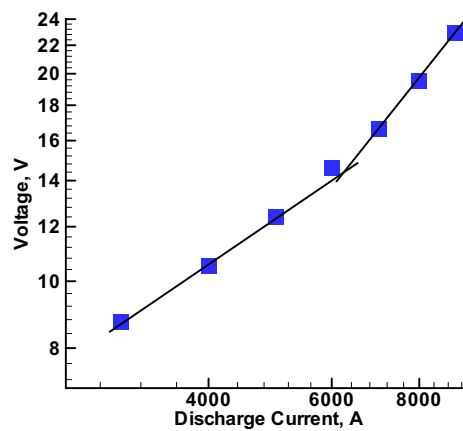


Figure 9. Voltage as a function of current (except the sheath drop)

Lorentz force is higher and absolute value of Joule heating is less likely to increase with rising current. In addition, since the current contour line expands toward the downstream with increasing current, the radial Lorentz force becomes higher. Then aerodynamic expansion tends to be suppressed. These facts seem to decrease the ratio of the aerodynamic thrust.

The specific impulse as a function of the current is depicted in Fig. 8. As the current increases, specific impulse rises up to 1870 s at  $J=9000$  A. When the current is equal to 9000 A, the  $J^2/\dot{m}$  parameter is  $1 \times 10^{11} \text{ A}^2/\text{kg/s}$ . In the these range of operation with argon, specific impulse is supposed to be about 2000 s,<sup>1</sup> so the result seems to be reasonable.

### G. Voltage

The discharge voltage is estimated by the line integral of the electric field from anode to cathode. Hence the voltage dose not include the sheath drop. Its plot as a function of the discharge current is depicted in Fig. 9 with double logarithmic plot. In general, as is well known, the slope of voltage plot changes to higher value at a certain current as the current is increased.<sup>16-17</sup> In this simulation, the change of slope is obtained around  $J=6000$  A. This fact suggests that the effect of the work done by the Lorentz force reveals above  $J=6000$  A. Therefore this result also shows that the acceleration mode changes into electromagnetic around  $J=6000$  A.

## H. Electron density along the anode

The performance of an MPD thruster is limited by the voltage oscillation referred as “onset”. When a flared anode is adopted like this study, it is supposed to occur the starvation of propellant along the anode as the discharge current is increased. The discharge current is equivalent to the flow of the charged particles, especially electrons. Since the electrons are produced from the ionization processes, its number density dose not seems to decrease monotonically as the current is increased. Therefore the electron number density has to be examined. Figures 10 and 11 show the electron number density and ionization fraction along the flared part of the anode depicted in Fig.1 as A-B as a function of axial coordinate. As the current is increased from 4000 to 6000 A, the electron number density rises all over the anode surface. There are two maximum points in the electron density plot. The left maximum point is caused by the ionization due to the high temperature around point A, which is understood from the ionization fraction plot increasing along the anode. The right one is produced by the compression wave from the cathode tip. These two effects keep the electron number density relatively constant along the anode. With the current increasing, the slope of the compression wave against the symmetric axis reduced, so the right maximum point moves toward the point B.

According to the Fig. 11, ionization fraction rapidly turns into higher value up to about 0.8 as the current increases from 6000 to 8000 A, and the ratio of increase also becomes higher with increasing current. However the electron number density decreases rapider along the anode as the current increases up to 8000 A. This rapid decrease seems to be caused by the strong Lorentz force toward downstream at the point A. Then the propellant itself tends not to inflow around the anode. This phenomenon suggests that the number of electrons along the anode runs short than the sufficient number to provide a given total current in the range of high current.

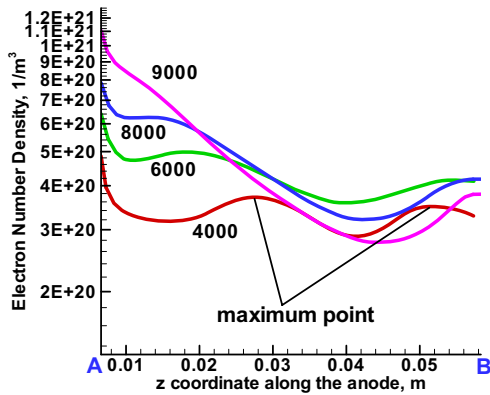


Figure 10. Electron Number Density along the flared part of the anode

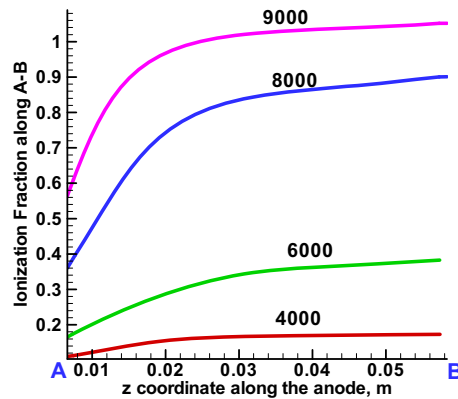


Figure 11. Ionization fraction along the flared part of the anode

## IV. Conclusions

Numerical analyses of a self-field MPD thruster considering non-equilibrium multiple ionization processes are conducted in order to examine the transition from aerodynamic acceleration to magnetic acceleration. Since the theoretical value of critical ionization current is about 6000 A, the discharge current  $J$  is changed from 3000 to 9000 A in the condition of constant mass flow rate 0.8 g/s.

The flow field at  $J=6000$  A, which corresponds to the critical ionization current, is discussed. The temperature distribution shows that the relative velocity between atoms and ions around the cathode tip is equivalent to the critical ionization velocity of argon. As to the ionization fraction distribution, the structure of cathode jet having high ionization fraction about 1.6 is obtained. For the examination of ionization progress with increasing current, mass fraction of Ar, Ar<sup>+</sup>, and Ar<sup>2+</sup> at a representative point is plotted as a function of the discharge current and then it is shown that the fraction of Ar<sup>+</sup> becomes dominant at  $J=6000$  A there.

As to the characteristics of thrust, the magnetic thrust exceeds aerodynamic thrust at  $J=6000$  A. In addition, the aerodynamic thrust begins to decrease at  $J=6000$  A while the magnetic thrust keeps to rise. Specific impulse increases with rising current up to 1870s at  $J=9000$  A.

The slope of the voltage plot as a function of discharge current with double logarithmic plot changes to higher value at  $J=6000$  A, which is often observed in many experiments.

As to the electron number density along the flared part of the anode, in the range of electrothermal acceleration, electron number density is relatively kept constant. However, in the range of electromagnetic acceleration, it decreases rapidly along the anode, and it is found that the single ionization progresses abruptly at the same time along the anode.

### Acknowledgment

This work has been supported by the Center for Planning and Information Systems in Institute of Space and Astronautical Science. We would like to gratefully acknowledge the members of Okuno laboratory in Tokyo Institute of Technology, and Funaki laboratory in Institute of Space and Astronautical Science.

### References

- <sup>1</sup>Sovey, J. S., Manteniaks, M. A., "Performance and Lifetime Assessment of Magnetoplasmadynamic Arc Thruster Technology," Journal of Propulsion and Power, Vol. 7, No. 1, 1991, pp. 71-83
- <sup>2</sup>Sankaran, K., Choueiri, E. Y., Jardin, S. C., "Comparison of Simulaed Magnetoplasmadynamic Thruster Flowfields to Experimental Measurements," Journal of Propulsion and Power, Vol. 21, No. 1, 2005, pp. 129-138
- <sup>3</sup>Heiermann, J., Auweter-Kurtz, M., "Numerical and Experimental Investigation of the Current Distribution in Self-Field Magnetoplasmadynamic Thrusters," Journal of Propulsion and Power, Vol. 21, No. 1, 2005, pp. 119-127
- <sup>4</sup>Mikellides, P. G., "Modeling and Analysis of a Megawatt-Class Magnetoplasmadynamic Thruster," Journal of Propulsion and Power, Vol. 20, No. 2, 2004, pp. 204-210
- <sup>5</sup>Niewood, E. H., Preble, J., Hastings, D. E., Martinez-Sanchez, M., "Electrothermal and modified two stream instabilities in MPD thrusters," AIAA paper 90-2607, July, 1990
- <sup>6</sup>Funaki, I., Toki, K., Kuriki, K., "Numerical Analysis of a Two-Dimensional Magnetoplasmadynamic Arcjet," Journal of Propulsion and Power, Vol. 13, No. 6, 1997, pp. 789-795
- <sup>7</sup>Nakata, D., Toki, K., Funaki, I., Shimizu, Y., Kuninaka, H., Arakawa, Y., "Experimental Verification For the Nozzle Shape Optimization of the Self-Field MPD Thruster," IEPC paper 2005-163, 2005
- <sup>8</sup>Takeda, H., Yamamoto, S. "Implicit Time-Marching Solution of Partially Ionized Flows in Self-Field MPD Thruster," Trans. Japan Soc. Aero. Space Sci., Vol. 44, No. 146, 2002, pp. 223-228
- <sup>9</sup>Sleziona, P. C., Auweter-Kurtz, M., Schrade, H. O., "Numerical Calculation of a Cylindrical MPD Thruster," IEPC paper,
- <sup>10</sup>Mitchner, M., Kruger, H., Jr., "Partially Ionized Gases," John Wiley and Son, New York, 1973
- <sup>11</sup>Lotz, W., "An Empirical Formula for the Electron-Impact Ionization Cross-Section," Zeitschrift für Physik, Vol. 206, 1967, pp. 205-211
- <sup>12</sup>Lotz, W., "Electron-Impact Ionization Cross-Sections and Ionization Rate Coefficients for Atoms and Ions from Hydrogen to Calcium," Zeitschrift für Physik, Vol. 216, 1968, pp. 241-247
- <sup>13</sup>Lotz, W., "Subshell Binding Energies of Atoms and Ions from Hydrogen to Zinc," Journal of the Optical Society of America, Vol. 58, No. 7, 1968, pp. 915-921
- <sup>14</sup>Tóth, G., Odstrčil, D., "Comparison of Some Flux Corrected Transport and Total Variation Diminishing Numerical Schemes for Hydrodynamic and Magnetohydrodynamic Problems," Journal of Computational Physics, Vol. 128, 1996, pp. 82-100
- <sup>15</sup>Yee, H. C., "A Class of High-Resolution Explicit and Implicit Shock-Capturing Methods," NASA TM-101088, 1989
- <sup>16</sup>Kuriki, K., Suzuki, H., "Transitional Behavior of MPD Arcjet Operation," AIAA Journal, Vol. 16, No. 10, 1978, pp. 1062-1067
- <sup>17</sup>Yoshikawa, T., Kagaya, Y., Kuriki, K., "Thrust and Efficiency of the K-III MPD Thruster," J. Spacecraft, Vol. 21, No. 5, 1984, pp. 481-487